Using earth observation-based dry season NDVI trends for assessment of changes in tree cover in the Sahel

Horion, Stéphanie; Fensholt, Rasmus; Tagesson, Torbern; Ehammer, Andrea

Published in:
International Journal of Remote Sensing

DOI:
10.1080/01431161.2014.883104

2014

Document Version:
Publisher's PDF, also known as Version of record

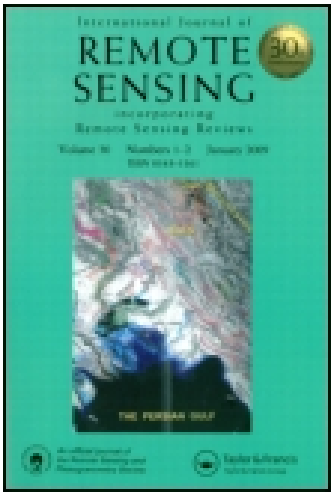

International Journal of Remote Sensing

Publication details, including instructions for authors and subscription information:
http://www.tandfonline.com/loi/tres20

Using earth observation-based dry season NDVI trends for assessment of changes in tree cover in the Sahel

Stéphanie Horion[a], Rasmus Fensholt[a], Torbern Tagesson[a] & Andrea Ehammer[a]

[a] Department of Geography and Geology, University of Copenhagen, DK-1350 Copenhagen, Denmark

Published online: 27 Mar 2014.

To cite this article: Stéphanie Horion, Rasmus Fensholt, Torbern Tagesson & Andrea Ehammer (2014) Using earth observation-based dry season NDVI trends for assessment of changes in tree cover in the Sahel, International Journal of Remote Sensing, 35:7, 2493-2515, DOI: 10.1080/01431161.2014.883104

To link to this article: http://dx.doi.org/10.1080/01431161.2014.883104

International Journal of Remote Sensing, 2014
Vol. 35, No. 7, 2493–2515, http://dx.doi.org/10.1080/01431161.2014.883104

Using earth observation-based dry season NDVI trends for assessment of changes in tree cover in the Sahel

Stéphanie Horion*, Rasmus Fensholt, Torbern Tagesson, and Andrea Ehammer

Department of Geography and Geology, University of Copenhagen, DK-1350 Copenhagen, Denmark

(*Received 29 November 2012; accepted 15 April 2013*)

The co-existence of trees and grasses is a defining feature of savannah ecosystems and landscapes. During recent decades, the combined effect of climate change and increased demographic pressure has led to complex vegetation changes in these ecosystems. A number of recent Earth observation (EO)-based studies reported positive changes in biological productivity in the Sahelian region in relation to increased precipitation, triggering an increased amount of herbaceous vegetation during the rainy season. However, this 'greening of the Sahel' may mask changes in the tree–grass composition, with a potential reduction in tree cover having important implications for the Sahelian population. Large-scale EO-based evaluation of changes in Sahelian tree cover is assessed by analysing long-term trends in dry season minimum normalized difference vegetation index ($NDVI_{min}$) derived from three different satellite sensors: Système Pour l'Observation de la Terre (SPOT)-VEGETATION (VGT), Terra Moderate Resolution Imaging Spectroradiometer (MODIS), and the Advanced Very High Resolution Radiometer (AVHRR) Global Inventory Modeling and Mapping Studies (GIMMS) dataset. To evaluate the reliability of using $NDVI_{min}$ as a proxy for tree cover in the Sahel, two factors that could potentially influence dry season $NDVI_{min}$ estimates were analysed: the total biomass accumulated during the preceding growing season and the percentage of burned area observed during the dry season. Time series of dry season $NDVI_{min}$ derived from low-resolution satellite time series were found to be uncorrelated to dry grass residues from the preceding growing season and to seasonal fire frequency and timing over most of the Sahel (88%), suggesting that $NDVI_{min}$ can serve as a proxy for assessing changes in tree cover. Good agreement ($R^2 = 0.79$) between significant $NDVI_{min}$ trends ($p < 0.05$) derived from VGT and MODIS was found. Significant positive trends in $NDVI_{min}$ were registered by both MODIS and VGT dry season $NDVI_{min}$ time series over the Western Sahel, whereas trends based on GIMMS data were negative for the greater part of the Sahel. EO-based trends were generally not confirmed at the local scale based on selected study cases, partly caused by a temporal mismatch between data sets (i.e. different periods of analysis). Analysis of desert area $NDVI_{min}$ trends indicates less stable values for VGT and GIMMS data as compared with MODIS. This suggests that trends in dry season $NDVI_{min}$ derived from VGT and GIMMS should be used with caution as an indicator for changes in tree cover, whereas the MODIS data stream shows a better potential for tree-cover change analysis in the Sahel.

1. Introduction

Time series of continuous Earth observation (EO)-based estimates of vegetation have significantly improved our understanding of intra- and inter-annual variations in vegetation from a regional to global scale (e.g. Myneni et al. 1997; Nemani et al. 2003;

*Corresponding author. Email: stephanie.horion@geo.ku.dk

Helldén and Töttrup 2008; Fensholt and Proud 2012). For dry-land areas such as the Sahel, EO-based analysis is particularly favourable because of the prevalence of cloud-free conditions (MEA 2005). In a climate change perspective, the Sahel is the region that has undergone the greatest variations in rainfall over the past 3–4 decades (Nicholson 2005). Since the 'Sahel drought' of the 1970s and early 1980s, this zone has been described as a hotspot of land degradation, threatened both by recurrent drought (Nicholson 2000) and human overuse (e.g. through overgrazing) (Lamb 1982; Nicholson 2000; Hulme 2001). Therefore, the region has been the subject of much EO-based research aiming at monitoring and uncovering the reason for these dramatic changes in vegetation cover and productivity. Tucker, Dregne, and Newcomb (1991) and Tucker and Nicholson (1999) found that the effects of the severe Sahelian drought in the mid-1980s were evident from time series of AVHRR (Advanced Very High Resolution Radiometer) data, showing a southward propagation of the Sahara desert. However, an almost total recovery in 1988 was also found, leading to the conclusion that no systematic increasing or decreasing trend of the size of the Sahara desert from 1980 to 1997 was evident. Anyamba and Tucker (2005) examined the AVHRR GIMMS (Global Inventory Modelling and Mapping Studies) time series 1981–2003 and found this 23-year period to include two different periods of opposite trends. 1982–1993 was marked by below-average normalized difference vegetation index (NDVI), while 1994–2003 was characterized by a trend towards conditions with region-wide above-normal NDVI conditions. A number of recent EO-based publications (Olsson, Eklundh, and Ardo 2005; Anyamba and Tucker 2005; Helldén and Töttrup 2008; Huber, Fensholt, and Rasmussen 2011; Kaspersen, Fensholt, and Huber Gharib 2011; Fensholt and Rasmussen 2011; Fensholt and Proud 2012) have pointed to the fact that the change of biological productivity in the Sahelian region is generally positive (the 'greening of the Sahel'). These studies indicate that there seems to be a strong correlation between rainfall conditions and biological productivity and that the narrative of irreversible degradation caused by increased population density and human overuse may not be valid as a general description of the Sahel.

However, if the observed greening is predominantly an effect of increased precipitation triggering an increased amount of herbaceous vegetation (annual grasses) during the rainy season, this may disguise continued 'degradation' caused by other factors, such as reduction in tree-cover density. People across the Sahel depend on trees for firewood, timber, and food, and an increased demand for wood has been reported by (Bächler 1998) caused by a dramatic increase in population density in the Sahel over the last decades. It is suggested that forest species richness, tree density, and forest carbon have declined in the past half-century as based on field research, local knowledge, aerial photos, and satellite data, suggesting widespread forest dieback or reductions in tree cover and biodiversity in response to drought and warmer temperatures in the African Sahel (Gonzalez, Tucker, and Sy 2012). The combined influence from increased aridity and human population is suggested to have reduced tree cover in parts of the African Sahel and degraded resources for local people (Poupon 1980; Gonzalez 2001; Wezel and Lykke 2006; Maranz 2009; Ruelland, Levavasseur, and Tribotté 2010).

These above-cited studies, no matter how thoroughly conducted including both village interviews and historical aerial photographs/very-high-resolution (VHR) satellite imagery, nevertheless suffer from the very limited footprint in time and space (few images covering multiple decades and tens to hundreds of square kilometres) when attempting to assess the status of ecosystem services such as firewood for an area such as the Sahel covering more than 3 million km^2.

An alternative EO-based approach for assessing changes in Sahelian tree-cover density is tested here using long-term time series of high-temporal Polar Operational Environmental Satellite (POES) NDVI data for a parameterization of the vegetation signal inherent in the dry season, where primarily changes in tree coverage will contribute to observed trends. The current study includes three different satellite sensor-based NDVI products spanning different periods: (1) NDVI data derived from the VEGETATION (VGT) sensor on board Système Pour l'Observation de la Terre (SPOT) and covering the period 1998–2011; (2) NDVI data derived from the Moderate Resolution Imaging Spectroradiometer (MODIS) on board Terra and covering the period 2000–2011; and (3) the AVHRR GIMMS dataset covering the period 1982–2011. We will first evaluate whether dry season NDVI can be used as a proxy for tree-cover density, as factors other than tree-cover density may influence dry season NDVI values, the most important being dry grass residues from the preceding growing season and frequency and timing of seasonal fires. An EO-based proxy for the total biomass accumulated during the preceding growing season and on fire occurrence will both be correlated to the dry season NDVI to assess the level of dependency between datasets. Consistency between across-sensor EO-derived dry season $NDVI_{min}$ trends is analysed for the Sahelian region and for a desert transect of no temporal change in $NDVI_{min}$. If consistency is found for an analysis of overlapping years (2000–2011), an assessment of trends in Sahelian tree-cover density covering the last three decades can be done based on the GIMMS NDVI time series analysis. Finally, trends will be compared to case studies reported in the scientific literature covering areas of known changes in tree-cover density including both negative changes (i.e. deforestation) and positive changes (i.e. reforestation or natural regeneration).

2. Data and methods

2.1. SPOT VGT 10-day composite NDVI

The ten-day synthesis product (S10) is a full-resolution product (1 km resolution) providing 10-day maximum value composite (MVC) NDVI (Holben 1986). The quality of S10 products is derived directly from the quality of P products (physical products). P products are top-of-atmosphere (TOA) products for which the inputs for atmospheric correction are provided. Atmospheric correction is performed based on the use of the SMAC algorithm (Rahman and Dedieu 1994), correcting for molecular and aerosol scattering, water vapour, and ozone and other gas absorption. Data inputs for the atmospheric correction of SPOT-VGT are aerosol optical depth (AOD), atmospheric water vapour, ozone (Maisongrande, Duchemin, and Dedieu 2004), and a digital elevation model for atmospheric pressure estimation (Passot 2000). Water vapour (six-hourly measurements) is obtained from Meteo-France in a 1.5° × 1.5° grid cell resolution. A climatology of ozone (based on multi-year Total Ozone Mapping Spectrometer (TOMS) observations) and AOD are provided by CESBIO (Centre d'Etudes Spatiales de la Biosphère). Aerosol optical depth is derived from the B0 band in combination with NDVI (Maisongrande, Duchemin, and Dedieu 2004), but prior to 2001, the AOD was a static data set that was only a function of latitude. P products are corrected for system errors (misregistration of the different channels, calibration of all the detectors along the line-array detectors for each spectral band) and resampled to a Plate-Carrée geographic projection (SPOT-VEGETATION User's Guide 2012). High absolute location and multi-temporal registration accuracy are obtained with an absolute location accuracy estimation

of 330 m RMS (Sylvander et al. 2000). Status maps are provided for each S10 product including per-pixel cloud cover information. The cloud flag information is based on thresholding of the TOA reflectance in each of the four bands, which are compared to reference reflectance maps for each band (Kempeneers, Lissens, and Fierens 2000; SPOT-VEGETATION User's Guide 2012).

This analysis is based on the recalibrated S10 product released in 2007, since an error was found in the SPOT-VGT instrument calibration scheme forcing the time series of the data acquired between 1 February 2003 and 31 May 2006 to be reprocessed (http://www.vgt.vito.be/pages/newcalibrationvgt2_final.pdf).

The SPOT satellites (SPOT 4 and SPOT 5) have an equator-crossing time of 10.30. The SPOT 4 and SPOT 5 satellite sensor design provides an improvement over the AVHRR scanning array with respect to spatial resolution distortion at off-nadir angles acquiring absence of distortion up to about 50° off-nadir (SPOT-VEGETATION User's Guide 2012). Furthermore, the SPOT-VGT instruments offer advantages over the AVHRR sensors, including better navigation and improved radiometric sensitivity (Gobron et al. 2000). The S10 products are available at http://free.vgt.vito.be/origin from SPOT 4 (VGT1 sensor) until January 2003, and after that from the SPOT 5 (VGT2 sensor). The spectral response functions (SRF) of the bands of SPOT 4 and SPOT 5 are not identical and can induce reflectance variations. For the near-infrared and red bands, a reflectance bias of 6.3% and 2.1% is found, respectively, producing an increase in observed NDVI of 3.4% (NDVI > 0.3) (http://www.vgt.vito.be/faqnew/index.html; question 5.1). Moreover, in a recent notification (http://www.spot-vegetation.com/pdf/Reflectance_communication_letter_V1.0.pdf), the Centre de Traitement d'Images VEGETATION (CTIV) mentioned that incorrect implementation of the standardization of solar illumination has been applied in the current VGT processing chain, having potential implications for the accuracy of time series analysis of VGT NDVI.

2.2. *MODIS 16-day composite NDVI data*

The sun-synchronous orbits of Terra and Aqua MODIS cross the dayside equator at 10:30 am and 1:30 pm local crossing time, with a 16-day repeat cycle. The MODIS instrument has a 110° across-track field of view and senses the entire equator every two days (Wolfe, Roy, and Vermote 1998). The MODIS NDVI 0.05° 16-day product (MOD13C1, Collection 5) is based on spatial averages of 16-day 1 km NDVI (MOD13A2) (Solano et al. 2010). MOD13A2 is processed from the MODIS level 2 (L2G) daily surface reflectance product (MOD09 series), which provides red and near-infrared surface reflectance corrected for the effect of atmospheric gases, thin cirrus cloud, and aerosols. The MOD09 band 1–7 product is an estimate of the surface spectral reflectance as would be measured at ground level if there were no atmospheric scattering or absorption (Vermote, El Saleous, and Justice 2002). Sensor degradation issues affecting particularly the blue band (B3, 470 nm) were recently reported for Terra MODIS Collection 5, with the largest impacts on simulated surface reflectance observed at near-nadir view angles (Wang et al. 2012).

2.3. *GIMMS 15-day composite NDVI product (GIMMS3g)*

The series of AVHRR instruments have a 110° across-track field of view allowing for near-daily global coverage. The GIMMS NDVI dataset is based on the GAC (Global Area Coverage) 1B product (Goward et al. 1993). GAC data were derived by onboard averaging and sampling of the 1.1 km full resolution data Local Area Coverage (LAC) to a

4 km resolution (Townshend 1994). For a given scan line, the first four pixels out of five are averaged and only every third scan line is processed, resulting in a nadir cell-size of 1.1 × 4 km with a gap of 2.2 km across the scan lines (Kidwell 1991). The channel 1 and 2 data used for the GIMMS data are calibrated as suggested by Vermote and Kaufman (1995), and the derived NDVI is further adjusted using the technique of Los (1998). The cloud detection algorithm is based on reflectance and brightness temperature values (Stowe et al. 1991; Tucker et al. 2005). No atmospheric correction is applied to the GIMMS data except for volcanic stratospheric aerosol periods (1982–1984 and 1991–1994) (Tucker et al. 2005). A satellite orbital drift correction is performed using the empirical mode decomposition/reconstruction (EMD) method of Pinzon, Brown, and Tucker (2005), minimizing effects of orbital drift by removing common trends between time series of solar zenith angle (SZA) and NDVI. The GIMMS3g NDVI data are provided in 1/12° resolution and processed to match the range of SPOT-VEGETATION and MODIS (Tucker et al. 2005), enabling the advantages of MODIS NDVI and VGT NDVI data to be used in conjunction with the historical information provided by the GIMMS dataset. For this study, bi-monthly GIMMS NDVI were used covering the period 1982–2011. This dataset originates from the NOAA AVHRR satellite series 7, 9, 11, 14, 16, 17, and 18, which are characterized by an afternoon overpass at launch, except for the NOAA-17, which has a morning overpass. NDVI quality flags are embedded in the 15-day maximum value compositing (Holben 1986) data files, providing information on per-pixel NDVI status identical to earlier versions of the GIMMS data. NDVI that are flagged as influenced by clouds or snow cover (flag = 1–5) are retrieved from either spline interpolation or average seasonal profiles, whereas flag = 0 indicates good value and flag 6 = missing data (Pinzon, Brown, and Tucker 2007). Only good-value GIMMS NDVI pixels are included in the current study.

2.4. *Ancillary data*

2.4.1. *MODIS MCD41 Burned Area Product*

The MODIS MCD45A1 Burned Area Product is a monthly Level 3 gridded product defining for each 500 m pixel the approximate day of burning (1–366) or providing a code indicating unburned areas, snow, water, or lack of data. The burned-area algorithm (Roy, Lewis, and Justice 2002, 2005) inverts a bi-directional reflectance model against multi-temporal land-surface reflectance observations (MODIS bands 2, 5, 6, and 7) recorded in a temporal window of 16 days to provide predicted reflectances and uncertainties of following observations over time. A statistical measure between the predicted and observed bi-directional surface reflectance is used to detect change from a previously observed state. The approximate day of burning is reportedly between eight days before and after the calendar month.

2.4.2. *Case study sites*

To assess whether trends derived from low-resolution satellite datasets were consistent with reported local changes in tree-cover density, we selected six case-study sites where changes in tree cover had been analysed by means of field survey, high-resolution imagery, and/or aerial photography (Figure 1 and Table 1). These sites were all located within the 150 and 700 mm isohyets delimiting the Sahelian region in this study, except for Sokolo (Mali), situated at the southern edge of the Sahel and characterized by higher

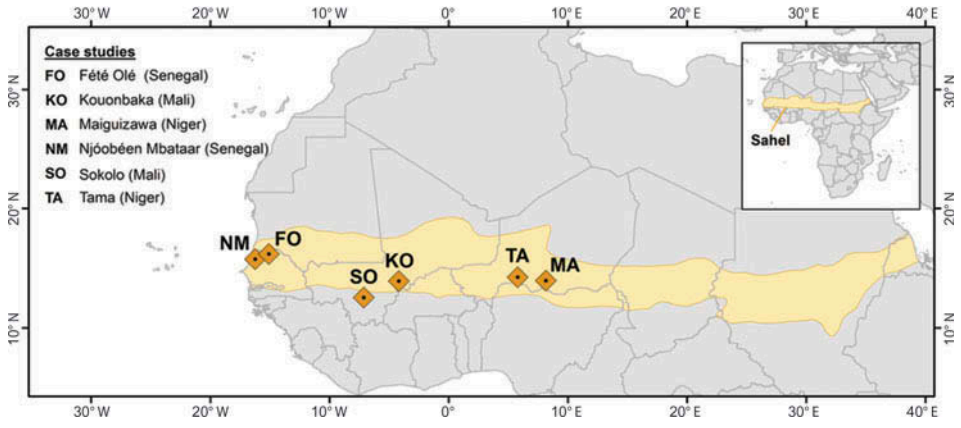

Figure 1. Delineation of the Sahelian region based on isohyets 150 and 700 mm and location of the case studies.

yearly precipitation (approx. 900 mm on average (1950–2000); Ruelland, Levavasseur, and Tribotté 2010). Negative changes in tree-cover density were reported in Njoobéen Mbataar (Senegal) and Fété Olé (Senegal) (Gonzalez, Tucker, and Sy 2012), and in Kouonbaka (Mali) and Sokoro (Mali) (Ruelland, Levavasseur, and Tribotté 2010), while Tama and Maiguizawa were characterized by a positive change in tree cover as a result of human intervention and natural regeneration (Larwanou and Saadou 2011; Abdoulaye and Ibro 2006).

Several criteria have led the selection of those case studies: (i) the potential to locate each site with relatively high accuracy; (ii) a minimal spatial extent of the area of interest covering at least one GIMMS pixel; and (iii) detailed description of the methodology used to analyse and discuss changes in tree-cover density. Each case study was located and vectorized as a polygon of 1 or more pixels matching the GIMMS spatial resolution. The vector layer was then used to extract spatio-temporal statistics of dry season NDVI trends for all three sensors.

2.5. Data post-processing and methodology

2.5.1. Estimation of NDVI metrics

NDVI metrics used in this study (e.g. dry season minimum NDVI ($NDVI_{min}$) and growing season small integral (SIN)) were computed from time series parameterization using a Savitsky–Golay filter available in TIMESAT software (Jonsson and Eklundh 2002, 2004). The Savitsky–Golay filter is a moving filter that fits values from a least squares fit to a polynomial (Jonsson and Eklundh 2004). The polynomial is fitted to data points within a moving window of a certain width and the width of the window affects both the degree of smoothing and the ability to follow rapid changes. The fitting is performed in several steps, allowing for an adaptation to the upper envelope of the NDVI curve based on different weights assigned to data points above and below the result of the previous steps (Jonsson and Eklundh 2004). TIMESAT is designed to parameterize the growing season signal and to be able to extract the seasonality data from the dry period in TIMESAT, all three data sets being inverted prior to the parameterization. The Savitsky–Golay functions were fitted to the inverted NDVI data sets using the following parameters in the

Table 1. Characteristics of the six study sites, including location, area, and tree-cover changes reported in the literature.

Site (country)	Location	Area (km^2)	Imagery (date)/field survey	Changes in tree-cover density (TCD) stated by the authors (ref.)	Reference
Njóobéen Mbataar (Senegal)	15.80° N, 16.25° W	20	Aerial photographs (February 1954); aerial photographs (March 1989); Ikonos (February 2002); field survey in 2002 and 2005	Sign. decrease in TCD (–18%) from 1954 to 2002	Gonzalez et al. (2012)
Fété Olé (Senegal)	16.23° N, 15.10° W	20	Aerial photographs (February to April 1954); Ikonos (February 2002); field survey in 2002 and 2005	Sign. decrease in TCD (–17%) from 1954 to 2002	Gonzalez et al. (2012)
Kouonbaka (Mali)	13° 56′ 30″ N, 4° 11′ 50″ W	90	Corona (December 1967); Landsat TM (December 1990); SPOT 5 (December 2003); field survey in 2006 and 2007	Reduction in woody covers (approx. –35%), replaced mainly by erosional surface and croplands; most changes occurred between 1967 and 1990	Ruelland, Levavasseur, and Tribotté (2010)
Sokoro (Mali)	12° 33′ 50″ N, 7° 8′ 12″ W	250	Corona (January 1967); Landsat TM (November 1986); SPOT 5 (December 2004); field survey in 2006 and 2007	Reduction in woody covers (approx. –34%), replaced mainly by croplands	Ruelland, Levavasseur, and Tribotté (2010)
Tama (Niger)	14° 16′ 30″ N, 5° 46′ 14″ E	Not mentioned	Field survey (exact date not mentioned)	Types of intervention: tree plantations and windbreaks (first intervention in 1975). Observed changes: high rate of regeneration (i.e. density of young sprouts) and of harvestable volumes	Larwanou and Saadou (2011) and Abdoulaye and Ibro (2006)
Maiguizawa (Niger)	13° 59′ 09″ N, 8° 08′ 45″ E	Not mentioned	Field survey (exact date not mentioned)	Type of intervention: tree plantations and windbreaks between 1985 and 1987, and farmer-managed natural regeneration (FMNR). Observed changes: high rate of regeneration (i.e. density of young sprouts) and of harvestable volumes.	Larwanou and Saadou (2011) and Abdoulaye and Ibro (2006)

TIMESAT analysis: seasonal parameter = 0.5, number of envelope iterations = 2, adaptation strength = 1, Savitzky–Golay window size = 2, amplitude season start and end = 20%.

Per-pixel dry season minimum NDVI ($NDVI_{min}$) and growing season small integral (SIN) were extracted from the three NDVI datasets (GIMMS bi-monthly NDVI; MODIS 16-day NDVI; VGT 10-day NDVI). In this study, $NDVI_{min}$ was used as a proxy for tree cover and, by extension, trends in $NDVI_{min}$ should inform on changes in tree cover in the Sahel.

2.5.2. *Estimation of yearly burned area percentage cover (BurnA) and date of first-registered burned area after growing season (BurnD)*

In this study, the MCD45A1 products were filtered for double events to avoid an overestimation of burned area counts, as there is a 16-day overlap period that allows a double registration of the same burning event. Yearly totals of burned area counts, as well as the date of the first burned area registered after the growing season, were extracted per pixel. The date 1 October was chosen as the starting day for the count as this corresponds to the approximate averaged end of the growing season in the Sahel. To account correctly for the timing of a burned area, original days of year (DOYs) were also converted to a new calendar with day 1 corresponding to 1 October, as a burned area registered on DOY 274 (1 October) of a given year is prior to a burned area registered on DOY 001 (1 January) of the following year. Per-pixel yearly burned area percentage covers (BurnA) were estimated by aggregating the 500 m information on burns counts to MODIS 0.05° spatial resolution. Similarly, the averaged date of the first-registered burned area after the growing season (BurnD) was derived at 0.05° resolution from the original 500 m MCD41 dataset.

2.5.3. *Trend estimation*

Trend analysis was carried out to estimate the magnitude and direction of changes in $NDVI_{min}$, starting from the hypothesis that changes in the vegetation signal during the dry season will primarily be influenced by changes in tree cover. Per-pixel temporal trends in the $NDVI_{min}$ datasets from SPOT-VGT, MODIS, and GIMMS were examined by applying a non-parametric linear regression model with time as the independent variable and $NDVI_{min}$ as the dependent variable. Analyses on both the full length of the individual datasets (14, 12, and 30 years respectively) and the period of overlap in time (2000–2011; $n = 11$) were performed. The outputs of the trend analyses are maps of regression slope values, indicating the strength and magnitude of the calculated trend. Since time series of NDVI often do not meet parametric assumptions of normality and homoscedasticity (Hirsch and Slack 1984), a median trend (Theil-Sen) procedure was applied. The Theil-Sen procedure is a method for robust linear regression that calculates the non-parametric slope and intercept of the series by determining the median of all estimates of the slopes derived from all pairs of observations (Hoaglin, Mosteller, and Tukey 2000). Non-parametric tests such as Theil-Sen (TS) are known to be robust against seasonality, non-normality, heteroscedasticity, and temporal autocorrelation (at both intra- and inter-annual scale) (Alcaraz-Segura et al. 2010; Hirsch and Slack 1984; Vanbelle and Hughes 1984) and are suggested for studies of vegetation trends based on time series of NDVI data (de Beurs and Henebry 2005). The TS procedure is

furthermore resistant to outliers and therefore suitable for assessing the rate of change in short or noisy series (Eastman et al. 2009).

The significance of $NDVI_{min}$ and BurnD time series trends was calculated by the non-parametric Mann–Kendall (MK) significance test. The MK significance test is commonly used as a trend test for the TS median slope operator (Eastman et al. 2009) and produces outputs of z-scores that allow for assessment of both the significance and direction of the trend. A positive slope ($z \geq 1.96$) represents a significant increase ($p < 0.05$) in dry season NDVI for the period 2000–2011, and negative slopes ($z \leq -1.96$) indicate a significant decrease ($p < 0.05$) over time.

2.5.4. Linear correlation analysis

Linear correlation analysis was performed to assess the strength of the linear association between datasets following two main rationales: (i) to assess whether $NDVI_{min}$ provides information on the dry season biomass that can be considered as independent from the herbaceous cover of the preceding growing season (as measured by SIN) and/or from the fire events registered during the dry season (as measured by BurnA); and (ii) to assess the goodness of fit between significant trends ($p < 0.05$) in $NDVI_{min}$ derived from GIMMS, MODIS, and VGT datasets.

In the first case, the per-pixel Pearson product moment correlation coefficient (r) was calculated between MODIS $NDVI_{min}$ and SIN for the 12-year time series (2000–2011) period, and between $NDVI_{min}$ and BurnA for the period 2001–2011, as the dry season burn counts for 2000 could not be completed.

In the second case, the linear association between dry season $NDVI_{min}$ trends derived from the different NDVI datasets was evaluated for the entire Sahel. Spatial resampling was applied to match the data when comparing slope coefficients derived from differently sized pixels (GIMMS 1/12°; MODIS 0.05°; VGT 1 km). VGT and MODIS slope coefficients were resampled to the least common denominator with the GIMMS pixels. Only resampled VGT and MODIS pixels that were covered by at least 3/4 of non-resampled pixels showing significant $NDVI_{min}$ slope coefficients were considered in the linear regression analysis. This was done by calculating the percentage cover of VGT and MODIS significant slopes ($p < 0.05$) within a GIMMS pixel as based on the z-score images.

3. Results

3.1. Correlations between minimum dry season NDVI ($NDVI_{min}$) and growing season small integral (SIN)/burned area percentage (BurnA)

Low correlations between dry season $NDVI_{min}$ and growing season small integral (SIN) were observed for the majority of pixels in the Sahel (pixels located between the isohyets 150 and 700 mm used in this study as delimitation for the Sahel) for the period 2000–2011 (Figure 2(*a*)). Only 8% of pixels had a Pearson correlation coefficient r significantly different from 0 at $p = 0.05$ ($|r| > 0.576$), indicating that, for a large majority of pixels in the Sahel, there is no significant relationship between the intensity of the growing season as measured by SIN and $NDVI_{min}$. Similarly no apparent relationship between $NDVI_{min}$ and BurnA was found at this scale of analysis (i.e. spatial resolution of 0.05°), as only 2% of the pixels over the Sahel presented significant r at $p = 0.05$ ($|r| > 0.604$) (Figure 2(*b*)). Figure 2(*c*) presents the per-pixel z-scores associated with the slope coefficients obtained

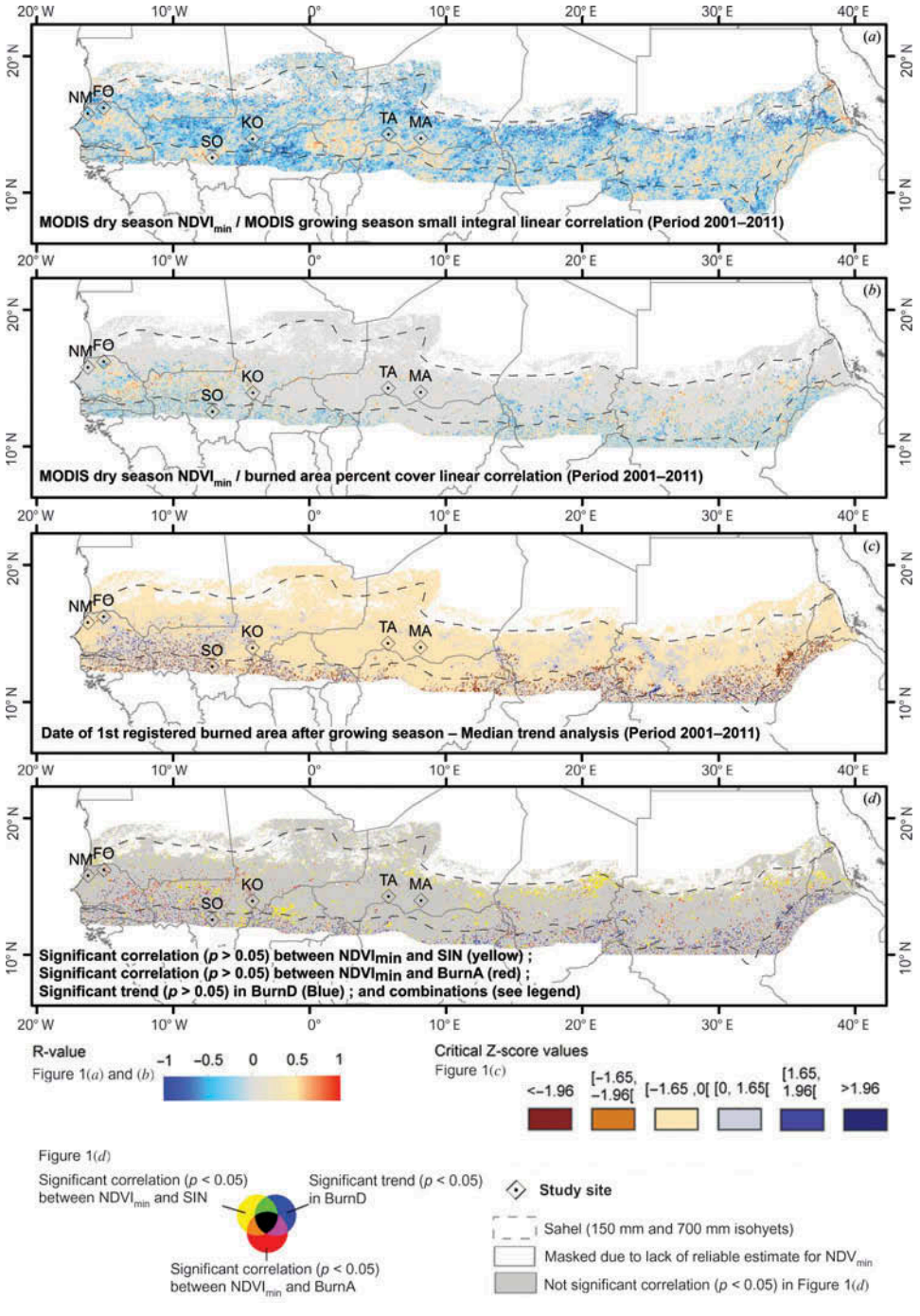

Figure 2. Correlation between dry season minimum NDVI ($NDVI_{min}$) and (*a*) growing season small integral (SIN) and (*b*) burned area percentage (BurnA); (*c*) *z*-scores associated with trend analysis based on the date of the first-registered burned area after the growing season (BurnA) (period 2001–2011) revealing (*d*) the location of pixels where the use of $NDVI_{min}$ as proxy for tree cover should be interpreted with caution. Absolute *z*-scores equal to or higher than 1.96 correspond to significant slope coefficients ($p < 0.05$).

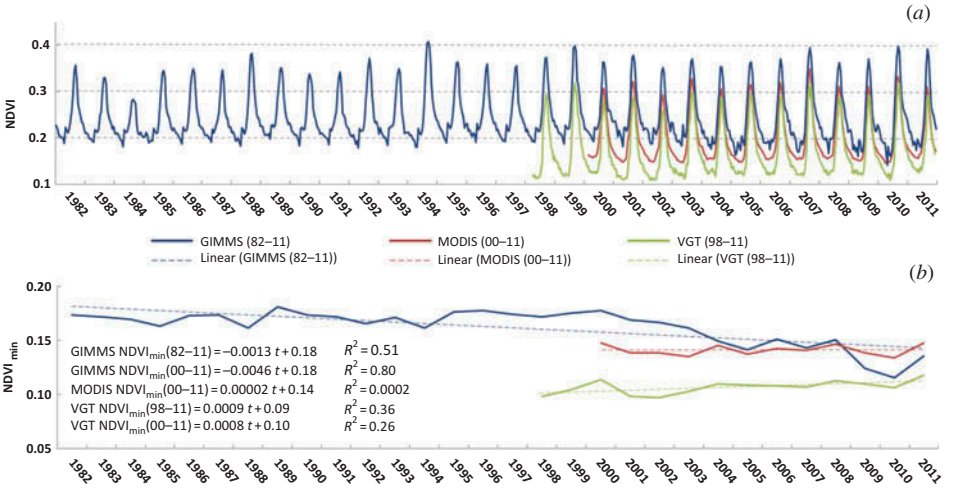

Figure 3. Spatially averaged time series for the Sahel: (*a*) 16-day MODIS, 10-day VEGETATION, and 15-day GIMMS3g NDVI; (*b*) yearly dry season minimum NDVI derived from the same sensors. The Sahelian region is delimited by the 150–700 mm isohyets.

for the date of the first-registered burned areas after the growing season (BurnD). Only a limited of number pixels showed significant trends (1.3% ($p < 0.05$) and 2.6% ($p < 0.1$), suggesting little change in the timing of the start of the fire season.

In total, pixels presenting a significant correlation ($p < 0.05$) with SIN and/or BurnA, and/or significant trend ($p < 0.05$) in BurnD covered less than 12% of the Sahelian region (Figure 2(*d*)). These results suggest that, for those pixels, changes in the total biomass accumulated during the preceding growing season and/or in seasonal fires explain part of the variability in the dry season $NDVI_{min}$, and therefore trends in $NDVI_{min}$ over these pixels were not investigated further.

3.2. GIMMS, MODIS, and VGT dry season $NDVI_{min}$ trends

Spatial averages of GIMMS, MODIS, and VGT NDVI (Figure 3(*a*)) and dry season minimum NDVI (Figure 3(*b*)) were calculated for pixels in the Sahel. From the visual comparison of NDVI time series for the different sensors (Figure 2(*a*)), $NDVI_{min}$ derived from the GIMMS dataset shows a decreasing tendency, especially since 2000, which is not present in the VGT and MODIS time series. The linear regression analysis performed on the Sahel integrated values of $NDVI_{min}$ confirmed that a significant negative trend ($\alpha = 0.05$) was registered for the GIMMS $NDVI_{min}$ at the Sahel scale (Figure 3(*b*)), while non-significant and significant positive trends were registered for the MODIS and VGT $NDVI_{min}$ time series, respectively. When fitting the regression models only for the sensor overlap period (2000–2011), the significant negative trend observed for the GIMMS $NDVI_{min}$ became stronger whereas both MODIS and VGT $NDVI_{min}$ presented non-significant trends.

Per-pixel dry season $NDVI_{min}$ trends calculated for the overlap period (2000–2011) are presented in Figure 4. Pixels are masked out based on: (i) slope values that were not significantly different from 0 ($p < 0.05$); (ii) pixels not indicating any clear seasonality according to TIMESAT; (iii) pixels for which the hypothesis of $NDVI_{min}$ as proxy for

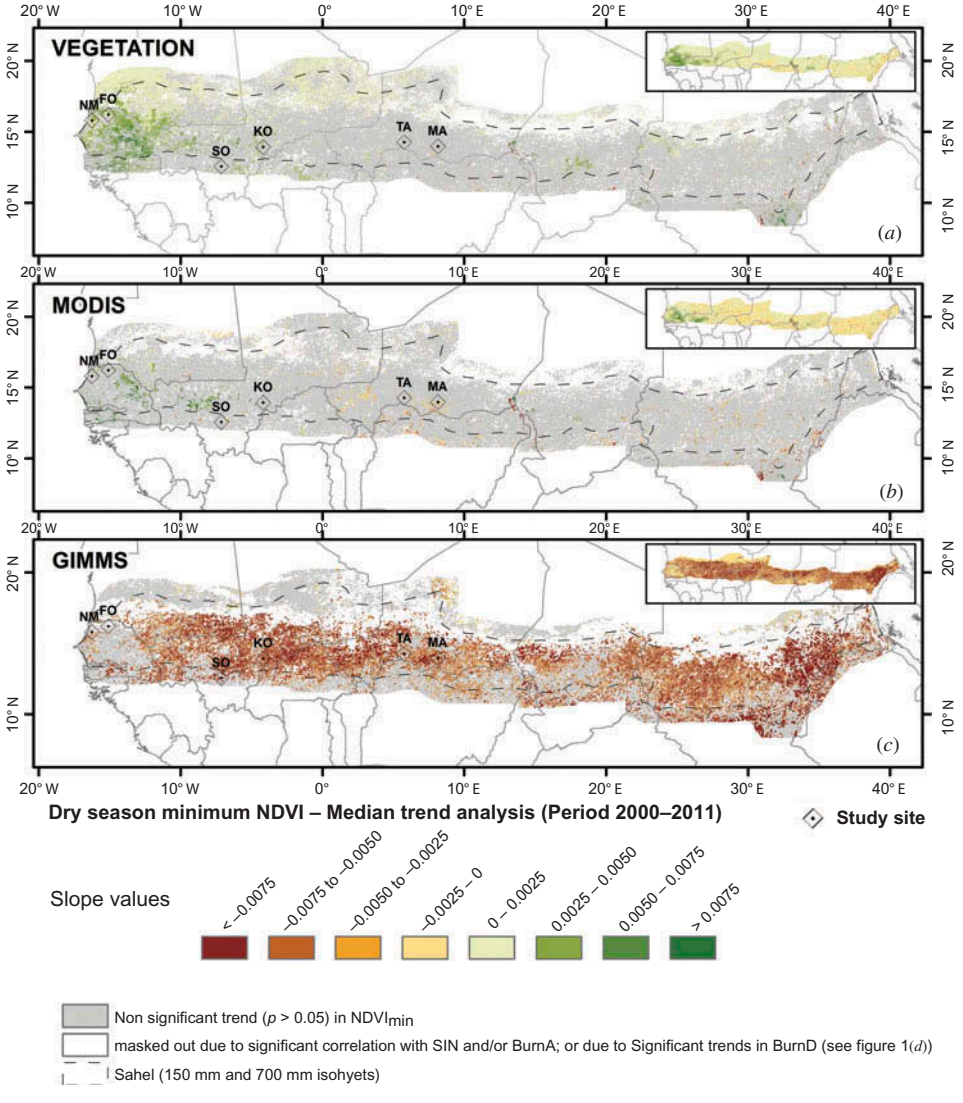

Figure 4. Dry season $NDVI_{min}$ trends for the overlap period 2000–2011 derived from (*a*) VGT, (*b*) MODIS, and (*c*) GIMMS. Slope coefficients not significantly different from zero ($\alpha = 0.05$) were masked out, as well as water bodies and pixels for which TIMESAT failed to extract dry season parameters. Both significant and non-significant slope coefficients are presented in a secondary frame placed at the top left of each main frame (*a*), (*b*), (*c*).

tree-cover density is not valid; and (iv) water bodies. Significant trends in VGT $NDVI_{min}$ were registered for 23.2% of the pixels in the Sahel (Figure 4(*a*)), with the largest positive trends observed in the western part (Senegal and in smaller proportions in South Mauritania and Mali) and in Chad. Significant trends in MODIS $NDVI_{min}$ were only observed for 7.4% of the pixels (Figure 4(*b*)), with positive signs in the Western Sahel and in Central Chad and negative signs in the rest of the Sahelian region. In comparison with VGT and MODIS, significant trends in GIMMS $NDVI_{min}$ were observed for a larger portion of the Sahel (59.7%), and were negative over the entire region.

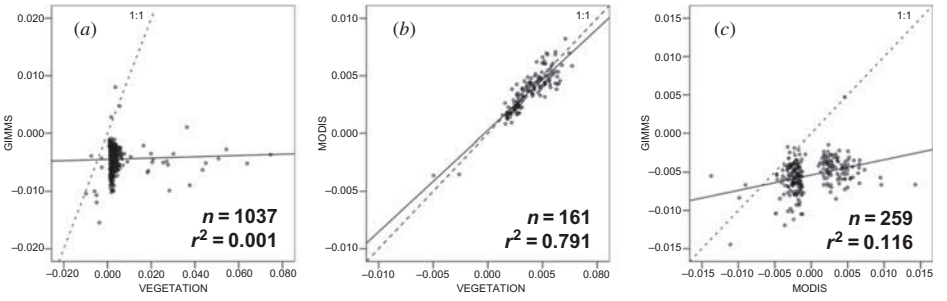

Figure 5. Correlation between dry season $NDVI_{min}$ slope coefficients resampled to GIMMS spatial resolution: (*a*) VEGETATION vs. GIMMS, (*b*) MODIS vs. GIMMS, and (*c*) VEGETATION vs. MODIS.

After resampling the VGT and MODIS slope coefficient products to the GIMMS resolution, the strength of linear association between the dry season $NDVI_{min}$ trends derived from GIMMS, MODIS, and VGT datasets was determined by calculating the Pearson product moment correlation coefficient (r) for the 12-year time series (2000–2011). Only significant trends ($p < 0.05$) were considered in the analysis. No good linear association is observed between the GIMMS $NDVI_{min}$ trends and the two other datasets (VGT and MODIS, Figures 5(*a*) and (*c*), respectively) for the pixels fulfilling the selection criteria (significant GIMMS slope coefficients; more than 75% of VGT/MODIS pixels ($p < 0.05$) before resampling to GIMMS resolution). The strongest linear association is observed between VGT $NDVI_{min}$ trends and MODIS $NDVI_{min}$ trends (Figure 5(b); $R^2 = 0.79$), with a slope close to the 1:1 line.

Per-pixel dry season $NDVI_{min}$ trends calculated from the full available archive period (GIMMS 1982–2011; VGT 1998–2011) are presented in Figure 6. Similar spatial patterns can be observed between the VGT $NDVI_{min}$ trends calculated for the overlap period (Figure 4(*a*)) and for the entire archive period (Figure 6(*a*)). The main difference resides in the number of pixels with significant slope coefficients, which increased from 23.2% for the overlap period to 31.8% for the entire archive period. Per-pixel GIMMS $NDVI_{min}$ trends calculated from the 30-year archive (Figure 6(*b*) showed negative trends over most of the Sahelian region, in line with the results obtained for the overlap period (2000–2011). However the values of the slope coefficients were generally smaller, indicating that the inclusion of the 1980s and 1990s in the analysis compensated for the trends observed during the 2000–2011 period. This result is in line with the observed average values at Sahel scale (Figure 3(*b*)).

3.3. *Trends analysis for desert transect*

The comparison of trend analysis results from different datasets for the overlapping period revealed that GIMMS $NDVI_{min}$ trends are systematically more negative than those derived from the MODIS and VGT NDVI datasets. Moreover, we observed a higher number of pixels with significant positive trends using the VGT NDVI data as compared with the MODIS NDVI data. To test whether $NDVI_{min}$ trends identified using these datasets may be influenced by sensor drift and/or calibration inaccuracies, we extracted the time profiles of $NDVI_{min}$ for a transect of approximately 4 × 360 GIMMS pixels located in the Sahara desert (between 8° W and 26° E, and centred on 20° 10′ N), where NDVI is not expected to change over time. It appeared that there is a distinct shift towards

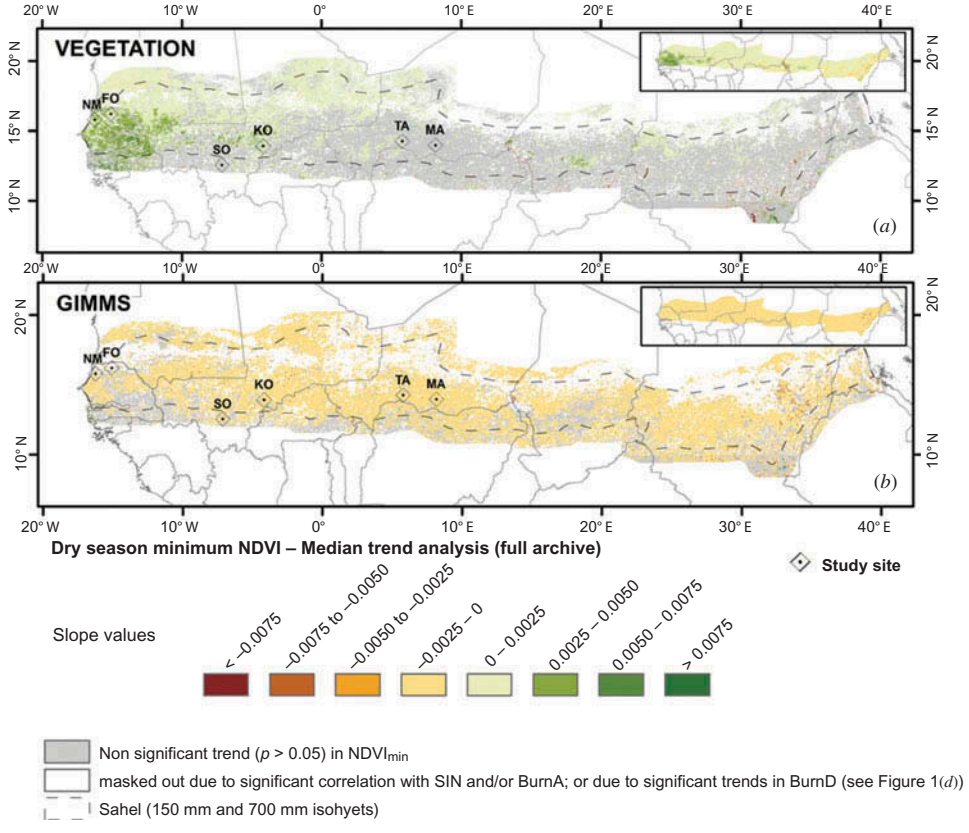

Figure 6. Dry season $NDVI_{min}$ trends for the full archive derived from (*a*) VGT (1998–2011), (*b*) MODIS (2000–2011), and (*c*) GIMMS (1982–2011). Slope coefficients not significantly different from zero ($\alpha = 0.05$) were masked out, as well as water bodies and pixels for which TIMESAT failed to extract dry season parameters. Both significant and non-significant slope coefficients are presented in a secondary frame placed at the top left of each main frame (*a*), (*b*), (*c*).

higher VGT $NDVI_{min}$ values between 2002 and 2003, which corresponds to the sensor switch from VGT 1 to VGT 2 (Figure 6). The GIMMS $NDVI_{min}$ time series also presented intra-annual variations in minimum NDVI that coincide relatively well with changes in NOAA sensors. Also the standard deviation in GIMMS $NDVI_{min}$ along the transect was found to be highest amongst the three products. In comparison with GIMMS and VGT, the temporal profile of MODIS $NDVI_{min}$ extracted for the desert transect remained relatively flat for the entire overlap period (2000–2011), even though a decrease in value of 0.0002 per year was observed.

3.4. *Comparison of GIMMS/MODIS/VGT dry season $NDVI_{min}$ for the case study sites*

No significant trend in BurnD (date of first-registered burned area) was observed in the case study sites, suggesting that changes in the timing of the first fire occurring after the growing season were not identified for the time period of analysis (2001–2011) (Table 2). In addition, no significant correlation between $NDVI_{min}$ and SIN/BurnA was observed in

Table 2. Summary of the statistical analysis results for the six study sites (from right to left): correlation coefficients obtained between $NDVI_{min}$ and growing season small integral (SIN); correlation coefficients obtained between $NDVI_{min}$ and burned area percentage (BurnA); slope coefficients resulting from median trends analysis of $NDVI_{min}$ for different datasets (GIMMS, MODIS, VGT) and period of analysis; slope coefficients resulting from median trends analysis of BurnD (date of the first-registered burned area after growing season). These scores correspond to spatially averaged values over the site area. Standard deviations and number of pixels included in the spatial average are reported between brackets.

	Pearson correlation coefficient (r) for $NDVI_{min}$ vs.		Slope coefficient	Slope coefficient for dry season $NDVI_{min}$				
Sites (country)	Growing season small integral, SIN (2000–2011)	% cover of burned area, BurnA (2001–2011)	Date of first burned area, BurnD (2001–2012)	GIMMS $NDVI_{min}$ (1982–2011)	GIMMS $NDVI_{min}$ (2000–2011)	MODIS $NDVI_{min}$ (2000–2011)	VGT $NDVI_{min}$ (1998–2011)	VGT $NDVI_{min}$ (2000–2011)
Njóobéen Mbataar (Senegal)	0.073 (+/–0.239; n = 6)	0.073 (+/–0.239; n = 6)	0.0 (+/–0.0; n = 6)	–0.0007** (+/–0.0001; n = 2)	–0.0021* (+/–0.0007; n = 2)	0.0010 (+/–0.0009; n = 6)	0.0022** (+/–0.0003; n = 162)	0.0025** (+/–0.0004; n = 162)
Fété Olé (Senegal)	–0.063 (+/–0.239; n = 6)	0.142 (+/–0.223; n = 6)	0.0 (+/–0.0; n = 6)	–0.0004 (+/–0.0001; n = 2)	–0.0010 (+/–0.0004; n = 2)	0.0005 (+/–0.0011; n = 6)	0.0021** (+/–0.0004; n = 171)	0.0019* (+/–0.0004; n = 171)
Kouonbaka (Mali)	–0.218 (+/–0.317; n = 2)	0.0 (+/–0.0; n = 2)	0.0 (+/–0.0; n = 2)	–0.0018** (+/–0.0; n = 1)	–0.0065** (+/–0.0; n = 1)	0.0001 (+/–0.0008; n = 2)	0.0010 (+/–0.0006; n = 100)	0.0008 (+/–0.0006; n = 100)
Sokoro (Mali)	0.387 (+/–0.072; n = 6)	0.091 (+/–0.341; n = 6)	–1.0285 (+/–2.519; n = 6)	–0.0014** (+/–0.00002; n = 2)	–0.0050* (+/–0.0028; n = 2)	–0.0020 (+/–0.0005; n = 6)	0.0002 (+/–0.0009; n = 190)	0.0012 (+/–0.0011; n = 190)
Tama (Niger)	0.01 (+/–0.358; n = 2)	–0.011 (+/–0.212; n = 2)	0.0 (+/–0.0; n = 2)	–0.0013** (+/–0.0; n = 1)	–0.0027 (+/–0.0; n = 1)	0.0001 (+/–0.0010; n = 2)	0.0014 (+/–0.0012; n = 81)	0.0008 (+/–0.0013; n = 81)
Maiguizawa (Niger)	–0.008 (+/–0.152; n = 4)	0.0 (+/–0.0; n = 4)	0.0 (+/–0.0; n = 4)	–0.0011 (+/–0.0; n = 1)	–0.0037 (+/–0.0; n = 1)	–0.0012 (+/–0.0006; n = 4)	0.0003 (+/–0.0004; n = 81)	–0.0006 (+/–0.0006; n = 81)

Notes: **Significant at 0.05; *Significant at 0.1.

the case study sites, indicating that $NDVI_{min}$ may be used as a proxy for tree cover in these cases.

Significant negative trends in GIMMS $NDVI_{min}$ between 1982 and 2011 were observed at all sites characterized by reported decreases in tree-cover density, except in Fété Olé (Senegal). Negative trends in $NDVI_{min}$ were also registered by the GIMMS $NDVI_{min}$ dataset in Tama (Niger), where increases in tree-cover density were reported by Larwanou and Saardou (2011). Trends in MODIS $NDVI_{min}$ (2000–2011) were not significant for any of the study sites, whereas VGT $NDVI_{min}$ exhibited significant positive trends between 1998 and 2011 in the Senegalese sites of Njóobéen Mbataar and Fété Olé.

In most HR/*in situ*-based studies used as reference for the case study site analysis, changes in tree cover were assessed analysing the relative changes in a given variable (i.e. tree-cover density or percentage of woody cover) between two or three dates (Table 1): Njóobéen Mbataar in 1954, 1989, and 2002; Fété Olé in 1954 and 2002; Kouonbaka in 1967, 1990, and 2003; and Sokoro in 1967, 1986, and 2004. Owing to the timing of the observations from these case study sites, it is only feasible to perform a comparison between HR/*in situ*-based studies and the GIMMS data. Table 3 presents the tree-cover changes reported by Gonzalez, Tucker, and Sy (2012) and by Ruelland, Levavasseur, and Tribotté (2010) for these sites. To assess the level of agreement between reported changes in tree cover and changes in $NDVI_{min}$ between two specific years, relative changes in GIMMS $NDVI_{min}$ were computed as $((NDVI)_{min,\ year2} - (NDVI)_{min,\ year1})/(NDVI)_{min,\ year1}$ (Table 3). Comparable scores were obtained for reported relative changes in tree cover and relative changes in GIMMS $NDVI_{min}$ when both year 1 and year 2 were included in the GIMMS archive. In Njóobéen Mbataar (Senegal), the 4% decline in tree-cover density between 1989 and 2002 (Gonzalez, Tucker, and Sy 2012) corresponded to a decrease of –4.4% in GIMMS $NDVI_{min}$. In Sokoro (Mali), the 10% decrease in wood-cover

Table 3. Relative changes in tree cover at the six selected sites as reported by HR-/field campaign-based study (described in Table 1) and corresponding relative changes in GIMMS $NDVI_{min}$. Periods of analysis without temporal mismatch between the HR-/field campaign-based relative changes and relative changes derived from the GIMMS data set are marked in bold.

Sites (country)	Reported relative changes in tree cover (%)		Relative changes in GIMMS $NDVI_{min}$ (%)
Njóobéen Mbataar (Senegal)	Variable: tree density (tree per ha) (Gonzalez, Tucker, and Sy 2012)	(1954–1989) –22	(1982–1989) +3.5
		(1989–2002) –4	**(1989–2002) –4.4**
		(1954–2002) –18	(1982–2002) –1.1
Fété Olé (Senegal)	Variable: tree density (tree per ha) (Gonzalez, Tucker, and Sy 2012)	(1954–2002) –17	(1982–2002) –14.5
Kouonbaka (Mali)	Variable: % of total woody cover (% of total study area) (Ruelland, Levavasseur, and Tribotté 2010)	(1967–1990) –29	(1982–1990) –5.6
		(1990–2003) –6	**(1990–2003) –0.1**
		(1967–2003) –35	(1982–2003) –5.7
Sokoro (Mali)	Variable: % of total woody cover (% of total study area) (Ruelland, Levavasseur, and Tribotté 2010)	(1967–1986) –24	(1982–1986) +2.4
		(1986–2004) –10	**(1986–2004) –18.5**
		(1967–2004) –34	(1982–2004) –16.5
Tama (Niger)	Not mentioned (Larwanou and Saadou 2011; Abdoulaye and Ibro 2006)	Positive change in tree cover	(1982–2002) –17.8
Maiguizawa (Niger)	Not mentioned (Larwanou and Saadou 2011; Abdoulaye and Ibro 2006)	Positive change in tree cover	(1982–2002) –19.1

percentage (including both open and closed woody cover classes) reported by Ruelland, Levavasseur, and Tribotté (2010) between 1986 and 2004 corresponded to a 18.5% decrease in GIMMS $NDVI_{min}$. For the other sites, the correspondence between the reported changes in tree cover and the relative changes in GIMMS $NDVI_{min}$ was less clear. We also noted that for both sites characterized by tree plantations and natural regeneration (Tama and Maiguizawa in Mali), GIMMS $NDVI_{min}$ showed marked negative values (<–17%) between 1982 and 2011.

4. Discussion

4.1. *Dry season $NDVI_{min}$ as proxy for tree-cover density*

Gonzalez, Tucker, and Sy (2012) argued that NDVI time series derived from LR-resolution satellite sensors cannot be used to analyse change in tree-cover density because of the pre-dominance of the grassland signal in the overall NDVI. This argument is indeed valid during the growing season, as the contribution of green leaf area from the herbaceous cover overrides the contribution of the green leaf area from the woody cover in that period (Archibald and Scholes 2007), justifying the need for very high-resolution imagery to detect individual trees. However, during the dry season the herbaceous cover enters a senescent phase leading to its complete (or close to complete) disappearance and during that period tree cover is therefore the major contributor to the 'total greenness' as registered by vegetation spectral indices such as NDVI. Even though the minimum NDVI has been used in land-cover studies as part of the variables enabling the distinction between land-cover types (De Fries et al. 1998), it has rarely been used as the main (or single) proxy of vegetation cover/dynamic. Wagenseil and Samimi (2007) found a close relationship between woody cover in Namibian savannahs and dry season NDVI curvature and minimum as derived from SPOT-VGT. They showed that leaf expansion is achieved by trees and shrubs prior to grasses, and therefore $NDVI_{min}$ was found to be a key parameter in the distinction between woody and grass-dominated areas.

In this study we tested the hypothesis that trend analysis of $NDVI_{min}$ could provide information on tree-cover changes in the Sahel. $NDVI_{min}$ typically occurred at the end of the dry season (Figure 3(*a*)) when most of the herbaceous cover has been decomposed. However, to ensure that the impact of dry grass residues from the preceding growing season on $NDVI_{min}$ values does not influence the following $NDVI_{min}$, correlation analysis between $NDVI_{min}$ and the growing season small integral (SIN) was conducted (Figure 2), indicating that, for a large part of the Sahelian region, $NDVI_{min}$ provides independent information on phytomass during the dry season. Seasonal vegetation fires are also known to play an important role in savannah ecosystems (e.g. Sankaran et al. 2005; Murphy and Bowman 2012). Burn scars can influence NDVI time series since fire scar results in most cases alter the visible-to-near-infrared surface reflectance ratio (Lentile et al. 2006). Hence, changes in fire occurrence can potentially influence the magnitude and direction of changes (trends) in $NDVI_{min}$. However, the analysis of trend in date of the first-registered burned area after the growing season suggested little change in the timing of the start of the fire season for the period 2001–2011. Moreover, the correlation analysis between MODIS $NDVI_{min}$ and burned area percentage over the period 2001–2011 did not reveal any clear linkage (negative or positive) between these two datasets, supporting the hypothesis that the yearly $NDVI_{min}$ time series is not influenced by fire occurrence/preceding growing season intensity, and can provide valuable information on tree cover for most of the Sahel.

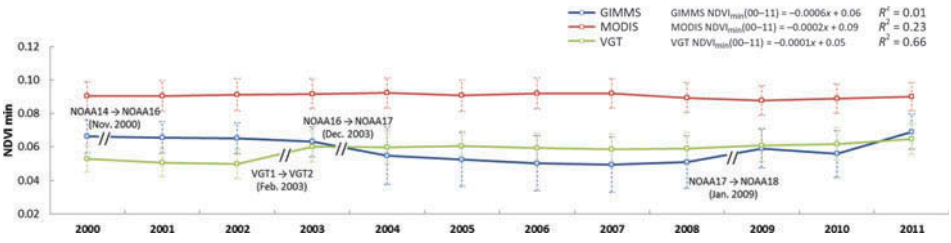

Figure 7. Time series of yearly dry season minimum NDVI spatially averaged over a desert transect for (*a*) MODIS, (*b*) VEGETATION, and (*c*) GIMMS3g. The desert transect covered 4 × 360 GIMMS pixels between 8° W and 26° E. Vertical bars represent the annual standard deviation along the transect.

4.2. Trends in dry season $NDVI_{min}$: consistency between GIMMS, MODIS, and VEGETATION datasets

Dry season $NDVI_{min}$ trends derived from MODIS and VGT NDVI datasets were found to be closer than those extracted from the GIMMS dataset for the overlap period (2000–2011) (Figures 4 and 5). Areas presenting positive trends in $NDVI_{min}$ were quasi-absent in the GIMMS dataset, while both the MODIS and VGT datasets showed areas in Senegal, Mali, and Niger with positive trends in $NDVI_{min}$. However, owing to reported problems in inter-sensor calibration and radiometric correction, determining an order of magnitude of changes in $NDVI_{min}$ remains challenging. Indeed the analysis of NDVI profiles extracted over a desert transect showed that there is a distinct shift towards higher VGT $NDVI_{min}$ values between 2002 and 2003, which corresponds to the sensor switch from VGT 1 to VGT 2 (Figure 7) characterized by different spectral response functions (http://www.vgt.vito.be/faqnew/index.html; question 5.1). We suspect this shift to be sufficiently important to influence the trend analysis results based on the SPOT-VGT datasets. Fensholt et al. (2009) pointed out that VGT1/VGT2 reflectance discrepancy may explain the higher positive trends in annual NDVI as compared with the MODIS annual NDVI. Moreover, the incorrect implementation of the standardization of solar illumination recently reported by the CTIV has a direct impact on the TOA values provided by VGT-P products (http://www.spot-vegetation.com/pdf/Reflectance_communication_letter_V1.0.pdf). The difference in reflectance values depends on the period of the year and can reach up to 6% in July. CTIV released a list of daily correction factors for the VGT-P time series. However, for VGT-S products providing top-of-canopy reflectance, the correction is not straightforward due to complex error propagation during the atmospheric correction and temporal compositing. The reprocessing of the entire archives is scheduled for the end of the VGT mission in order to avoid disruption of operational applications based on VGT time series analysis. This problem may impact trend analysis results, but no indication and/or error estimate have been provided so far by the CTIV that could help to discard or confirm results derived from such multi-annual analysis. In this particular study, we are focusing on the minimum NDVI values derived from VGT-S10 products. Knowing that the minimum value occurs during the dry season, the main source of error in the VGT-S10 used in our study should be linked to the total aerosol content in the atmosphere, as the cloud cover is almost non-existent during that period of the year. Moreover, as we are not using time-integrated values of NDVI (i.e. sum) but single date values ($NDVI_{min}$ based on MVC), we avoided accumulating errors over a long period of time.

GIMMS $NDVI_{min}$ time series also presented inter-annual variations in minimum NDVI coinciding with changes in NOAA sensors. However it is more difficult to estimate the magnitude and direction of $NDVI_{min}$ changes in this case (as compared to SPOT-VGT) due to the higher number of satellites/sensors that were used to build the GIMMS dataset and to the nature of the processing including EDM that theoretically should alleviate differences in SRFs and orbital drift between sensors.

Radiometric calibration issues in the MODIS Collection 5 were also reported by Wang et al. (2012). These authors showed that, for boreal forest and tundra in North America, negative NDVI trends up to –0.004 per year can be attributed to inaccurate correction of sensor degradation. Despite this calibration problem, which could result in negatively biased trends in NDVI, the $NDVI_{min}$ trends derived from MODIS appeared to be the most reliable based on the desert transect analysis. Wang et al. (2012) also indicated that Terra MODIS Collection 6 (available in the near future) should largely eliminate this negative bias. Further analysis will be needed to confirm the consistency of these trends.

4.3. Consistency between local changes in tree-cover density registered by field survey, HR, and LR imagery

Field survey- and high-resolution (HR)-based analyses of tree-cover changes are an extremely valuable support for discussing trend analysis results based on low-resolution (LR) satellite datasets. However, they are often based on a very limited number of images (two or three in the case of our case studies), which does not allow the accurate analysis of continuous trends in tree-cover density. Indeed, because research findings are driven by the acquisition dates of the images, a large part of the temporal evolution (or inter-annual variability) of the tree cover at a given site remains unknown.

Direct correspondence between changes in tree-cover density based on field survey and/or HR imagery and trends based on LR imagery (GIMMS, MODIS, and VGT) could not be found in any of the six case studies. A major reason is that most of the changes in tree-cover density reported by Ruelland, Levavasseur, and Tribotté (2010) and Gonzalez, Tucker, and Sy (2012) occurred prior to the VGT and MODIS era and therefore these studies cannot inform on the change in tree-cover density for the period 2000–2011. In the case of Tama (Niger), trees have been planted and protected for more than two decades, the first intervention being in 1975 (Abdoulaye and Ibro 2006). Moreover these authors reported that fast-growing species were used, which can explain that, despite the positive changes in tree cover reported by field surveys, no positive trends in $NDVI_{min}$ were registered by either MODIS or VGT datasets.

5. Conclusions

This study investigated the use of dry season $NDVI_{min}$ derived from low-resolution satellite imagery as proxy to assess long-term change in tree-cover density in the Sahel. Three datasets derived from different sensors and spanning different periods were evaluated: GIMMS AVHRR (1982–2011), SPOT-VGT (1998–2011), and Terra MODIS (2000–2011). The influence of dry grass residues from the preceding growing season and of changes in seasonal fires (area and timing) on $NDVI_{min}$ values were analysed to assess the performance of dry season NDVI as proxy for woody cover. Trends in $NDVI_{min}$ derived from the different datasets were then compared and case study sites were used to assess the consistency between trends in tree cover derived from LR imagery and HR imagery-/field campaign-based change analysis. It is concluded that dry season

$NDVI_{min}$ derived from LR satellite time series is influenced neither by dry grass residues from the preceding growing season nor from seasonal fires for most of the pixels in the Sahelian region. This suggests that the $NDVI_{min}$ can serve as a proxy for assessing changes in tree cover in the Sahel. Over the Western Sahel, significant positive trends in $NDVI_{min}$ were registered by both MODIS and VGT dry season $NDVI_{min}$ time series. These positive trends were not confirmed at the local scale based on the selected study cases due a temporal mismatch in the data comparison between tree-cover *in situ* records and VGT/MODIS datasets. Moreover, pre-processing issues were identified for all datasets (GIMMS, VGT, and MODIS), with larger and/or more complex impacts on $NDVI_{min}$ observed for GIMMS and VGT datasets, suggesting that trends in dry season $NDVI_{min}$ derived from these datasets as a proxy for tree cover should be used with caution. Further work will focus on quality assessment of identified $NDVI_{min}$ trend patterns using a larger set of study cases if possible, and more specifically on the identification and distinction of factors responsible for co-variation in the $NDVI_{min}$ time series and originating from natural (e.g. tree–grass distinction during the dry season), anthropic (e.g. population pressure, projects involving tree plantation and farmer-managed natural regeneration), and/or sensor-based phenomena.

Acknowledgements

The author thanks SpotImage/VITO for sharing the MODIS Land and SPOT VEGETATION data. The NASA Global Inventory Modeling and Mapping Studies (GIMMS) group is thanked for producing and sharing the GIMMS3g NDVI dataset. The NASA/MODIS Land Discipline Group is thanked for sharing the MODIS Land data.

Funding

This research is part of the project entitled 'Earth Observation based Vegetation Productivity and Land Degradation Trends in Global Drylands', funded by the the Danish Council for Independent Research (DFF) Sapere Aude programme.

References

Abdoulaye, T., and G. Ibro. 2006. *Analyse Des Impacts Socio-Économiques Des Investissements Dans La Gestion Des Ressources Naturelles: Etude De Cas Dans Les Régions De Maradi, Tahoua Et Tillabéry (Niger)*. Niamey: Centre Régional D'enseignement Spécialisé En Agriculture, Université Abdou Moumouni.

Alcaraz-Segura, D., E. Liras, S. Tabik, J. Paruelo, and J. Cabello. 2010. "Evaluating the Consistency of the 1982–1999 NDVI Trends in the Iberian Peninsula Across Four TIME SERIES Derived From the AVHRR Sensor: LTDR, GIMMS, FASIR, and PAL-II." *Sensors* 10 (2): 1291–1314.

Anyamba, A., and C. J. Tucker. 2005. "Analysis of Sahelian Vegetation Dynamics Using NOAA-AVHRR NDVI Data From 1981–2003." *Journal of Arid Environment* 63: 596–614.

Archibald, S., and R. J. Scholes. 2007. "Leaf Green-up in a Semi-Arid African Savannah –Separating Tree and Grass Responses to Environmental Cues." *Journal of Vegetation Science* 18: 583.

Bächler G, ed. 1998. "Violence Through Environmental Discrimination." *Causes, Rwanda Arena, and Conflict Model*. Dordrecht: Kluwer Academic Publishers.

de Beurs, K. M., and G. M. Henebry. 2005. "Land Surface Phenology and Temperature Variation in the International Geosphere–Biosphere Program High-Latitude Transects." *Global Change Biology* 11: 779–790.

De Fries, R. F., M. Hansen, J. R. G. Townshed, and R. Sohlberg. 1998. "Global Land Cover Classifications at 8 Km Spatial Resolution: The Use of Training Data Derived From Landsat

Imagery in Decision Tree Classifiers." *International Journal Remote Sensing* 19 (16): 3141–3168.
Eastman, J. R., F. Sangermano, B. Ghimire, H. L. Zhu, H. Chen, N. Neeti, Y. Cai, E. A. Machado, and S. C. Crema. 2009. "Seasonal Trend Analysis of Image Time Series." *International Journal of Remote Sensing* 30: 2721–2726.
Fensholt, R., and S. R. Proud. 2012. "Evaluation of Earth Observation Based Global Long Term Vegetation Trends – Comparing GIMMS and MODIS Global NDVI Time Series." *Remote Sensing of Environment* 119: 131–147.
Fensholt, R., and K. Rasmussen. 2011. "Analysis of Trends in the Sahelian 'rain-Use Efficiency' Using GIMMS NDVI, RFE and GPCP Rainfall Data." *Remote Sensing of Environment* 115: 438–451.
Fensholt, R., K. Rasmussen, T. T. Nielsen, and C. Mbow. 2009. "Evaluation of Earth Observation Based Long Term Vegetation Trends – Intercomparing NDVI Time Series Trend Analysis Consistency of Sahel From AVHRR GIMMS, Terra MODIS and SPOT VGT Data." *Remote Sensing of Environment* 113 (9): 1886–1898.
Gobron, N., B. Pinty, M. M. Verstraete, and J. L. Widlowski. 2000. "Development of Spectral Indices Optimized for the VEGETATION Instrument." Proceedings of VEGETATION 2000. Belgirate, April 3–6, 275–280.
Gonzalez, P. 2001. "Desertification and a Shift of Forest Species in the West African Sahel." *Climate Research* 17: 217–228.
Gonzalez, P., C. J. Tucker, and H. Sy. 2012. "Tree Density and Species Decline in the African Sahel Attributable to Climate." *Journal of Arid Environments* 78: 55–64.
Goward, S. N., D. G. Dye, S. Turner, and J. Yang. 1993. "Objective Assessment of the NOAA Global Vegetation Index Data Product." *International Journal of Remote Sensing* 14: 3365–3394.
Helldén, U., and C. Töttrup. 2008. "Regional Desertification: A Global Synthesis." *Global and Planetary Change* 64 (3–4): 169–176.
Hirsch, R. M., and J. R. Slack. 1984. "A Nonparametric Trend Test for Seasonal Data with Serial Dependence." *Water Resources Research* 20: 727–732.
Hoaglin, D. C., F. Mosteller, and J. W. Tukey. 2000. *Understanding Robust and Exploratory Data Analysis*. New York: Wiley.
Holben, B. N. 1986. "Characteristics of Maximum-Value Composite Images from Temporal AVHRR Data." *International Journal of Remote Sensing* 7: 1417–1434.
Huber, S., R. Fensholt, and K. Rasmussen. 2011. "Water Availability as the Driver of Vegetation Dynamics in the African Sahel from 1982 to 2007." *Global Planet Change* 76: 186–195.
Hulme, M. 2001. "Climatic Perspectives on Sahelian Desiccation: 1973–1998." *Global Environmental Change* 11: 19–29.
Jonsson, P., and L. Eklundh. 2002. "Seasonality Extraction by Function Fitting to TIME SERIES of Satellite Sensor Data." *IEEE Transactions on Geoscience and Remote Sensing* 40: 1824–1832.
Jonsson, P., and L. Eklundh. 2004. "TIMESAT – A Program for Analyzing TIME SERIES of Satellite Sensor Data." *Computers & Geosciences* 30: 833–845.
Kaspersen, P., R. Fensholt, and S. Huber Gharib. 2011. "A Spatio-Temporal Analysis of Climatic Drivers for Observed Changes in Sahelian Vegetation Productivity 1982–2007." *International Journal of Geophysics* 2011: 1–14.
Kempeneers, P., G. Lissens, and F. Fierens. 2000. "Development of a Cloud, Snow and Cloud Shadow Mask for VEGETATION Imagery." Proceedings of Vegetation 2000, 2 Years of operation to prepare the future, Belgirate, April 3–6, 303–306.
Kidwell, K. B. 1991. *NOAA Polar Orbiter Data User's Guide*. Washington, DC: NCDC/SDSD, National Climatic Data Center.
Lamb, P. J. 1982. "Persistence of Sub-Saharan Drought." *Nature* 299: 46–48.
Larwanou, M., and M. Saadou. 2011. "The Role of Human Interventions in Tree Dynamics and Environmental Rehabilitation in the Sahel Zone of Niger." *Journal of Arid Environments* 75: 194–200.
Lentile, L. B., Z. A. Holden, A. M. S. Smith, M. J. Falkowski, A. T. Hudak, P. Morgan, P. E. Gessler, S. A. Lewis, and N. C. Benson. 2006. "Remote Sensing Techniques to Assess Active Fire and Post-Fire Effects." *International Journal of Wildland Fire* 15 (3): 319–345.

Los, S. O. 1998. "Estimation of the Ratio of Sensor Degradation between NOAA AVHRR Channels 1 and 2 From Monthly NDVI Composites." *IEEE Transactions on Geoscience and Remote Sensing* 36: 206–213.
Maisongrande, P., B. Duchemin, and G. Dedieu. 2004. "An Operational Mission for the Earth Monitoring: Presentation of New Standard Products." *International Journal of Remote Sensing* 25: 9–14.
Maranz, S. 2009. "Tree Mortality in the African Sahel Indicates an Anthropogenic Ecosystem Displaced by Climate Change." *Journal of Biogeography* 36: 1181–1193.
Millennium Ecosystem Assessment (MEA). 2005. *Ecosystems and Human Well-Being: Desertification Synthesis*. Washington, DC: World Resources Institute.
Murphy, B. P., and D. M. J. S. Bowman. 2012. "What Controls the Distribution of Tropical Forest and Savanna?" *Ecology Letters* 15 (7): 748–758.
Myneni, R. B., C. D. Keeling, C. J. Tucker, G. Asrar, and R. R. Nemani. 1997. "Increased Plant Growth in the Northern High Latitudes from 1981 to 1991." *Nature* 386: 698–702.
Nemani, R. R., C. D. Keeling, H. Hashimoto, M. Jolly, S. W. Running, S. C. Piper, C. J. Tucker, and R. Myneni. 2003. "Climate Driven Increases in Terrestrial Net Primary Production from 1982 to 1999." *Science* 300: 1560–1563.
Nicholson, S. E. 2000. "The Nature of Rainfall Variability Over Africa on Time Scales of Decades to Millenia." *Global Planet Change* 26: 137–158.
Nicholson, S. E. 2005. "On the Question of the "Recovery" of the Rains in the West African Sahel." *Journal of Arid Environments* 63: 615–641.
Olsson, L., L. Eklundh, and J. Ardo. 2005. "A Recent Greening of the Sahel – Trends, Patterns and Potential Causes." *Journal of Arid Environement* 63: 556–566.
Passot, X. 2000. "VEGETATION Image Processing Methods in the CTIV." Proceedings of VEGETATION 2000: 2 years of operation to prepare the future. International Conference of VEGETATION 2000, edited by G. Saint, Lake Maggiore, April 3–6.
Pinzon, J., M. E. Brown, and C. J. Tucker. 2005. "Satellite Time Series Correction of Orbital Drift Artifacts Using Empirical Mode Decomposition." In *Hilbert-Huang Transform: Introduction and Applications*, edited by N. Huang, 167–186. Singapore: World Scientific.
Pinzon, J. E., M. E. Brown, and C. J. Tucker. 2007. *Global Inventory Modeling and Mapping Studies (GIMMS) Satellite Drift Corrected and NOAA-16 Incorporated Normalized Difference Vegetation Index (NDVI), Monthly 1981–2006*. Accessed January 2014. http://www.glcf.umd.edu/library/guide/GIMMSdocumentation_NDVIg_GLCF.pdf
Poupon, H. 1980. *Structure Et Dynamique De La Strate Ligneuse D'une Steppe Sahélienne Au Nord Du Sénégal*. Paris: Office de la Recherche Scientifique et Technique Outre-Mer.
Rahman, H., and G. Dedieu. 1994. "SMAC: A Simplified Method for the Atmospheric Correction of Satellite Measurements in the Solar Spectrum." *International Journal of Remote Sensing* 15: 123–143.
Roy, D. P., Y. Jin, P. E. Lewis, and C. O. Justice. 2005. "Prototyping a Global Algorithm for Systematic Fire-Affected Area Mapping Using MODIS Time Series Data." *Remote Sensing of Environment* 97: 137–162.
Roy, D. P., P. E. Lewis, and C. O. Justice. 2002. "Burned Area Mapping Using Multi-Temporal Moderate Spatial Resolution Data – A Bi-Directional Reflectance Model-Based Expectation Approach." *Remote Sensing of Environment* 83: 263–286.
Ruelland, D., F. Levavasseur, and A. Tribotté. 2010. "Patterns and Dynamics of Land-Cover Changes Since the 1960s Over Three Experimental Areas in Mali." *International Journal of Applied Earth Observation and Geoinformation*. 12S S11–S17.
SPOT-VEGETATION User's Guide. 2012. Accessed October 2012. http://www.spot-vegetation.com/userguide/userguide.htm
SPOT-VEGETATION FAQ (frequently asked questions). "FAQ 5.1." Accessed October 2012. http://www.vgt.vito.be/faqnew/index.html
Sankaran, M., N. P. Hanan, R. J. Scholes, J. Ratnam, D. J. Augustine, B. S. Cade, J. Gignouxet al. 2005. "Determinants of Woody Cover in African Savannas." *Nature* 438: 846–849.
Solano, R., K. Didan, A. Jacobson, and A. Huete. 2010. *MODIS Vegetation Indices (MOD13) C5 User's Guide*. Accessed January 2014. http://vip.arizona.edu/documents/MODIS/MODIS_VI_UsersGuide_01_2012.pdf
Stowe, L. L., E. P. McClain, R. Carey, P. Pellegrino, G. G. Gutman, P. Davis, C. Long, and S. Hart. 1991. "Global Distribution of Cloud Cover Derived From NOAA/AVHRR Operational Satellite Data." *Advances in Space Research* 3: 51–54.

Sylvander, S., P. Henry, C. Bastien-Thiry, F. Meunier, and D. Fuster. 2000. "VEGETATION Geometrical Image Quality." In *Proceedings of the VEGETATION 2000 Conference*, Belgirate, April 3–6, *CNES*, edited by G. Saint, 33–44. Ispra: Toulouse & JRC.

Townshend, J. R. G. 1994. "Global Data Sets for Land Applications from the Advanced Very High Resolution Radiometer: And Introduction." *International Journal of Remote Sensing* 15 (17): 3319–3332.

Tucker, C. J., H. E. Dregne, and W. W. Newcomb. 1991. "Expansion and Contraction of the Sahara Desert from 1980 to 1990." *Science* 253: 299–301.

Tucker, C. J., and S. N. Nicholson. 1999. "Variation in the Size of the Sahara Desert from 1980 to 1997." *Ambio* 28: 587–591.

Tucker, C. J., J. E. Pinzon, M. E. Brown, D. A. Slayback, E. W. Pak, R. Mahoney, E. Vermote, and N. El Saleous. 2005. "An Extended AVHRR 8-Km NDVI Dataset Compatible with MODIS and SPOT Vegetation NDVI Data." *International Journal of Remote Sensing* 26: 4485–4498.

Vanbelle, G., and J. P. Hughes. 1984. "Nonparametric-Tests for Trend in Water-Quality." *Water Resources Research* 20: 127–136.

Vermote, E., and Y. J. Kaufman. 1995. "Absolute Calibration of AVHRR Visible and Near Infrared Channels Using Ocean and Cloud Views." *International Journal of Remote Sensing* 16: 2317–2340.

Vermote, E. F., N. Z. El Saleous, and C. O. Justice. 2002. "Atmospheric Correction of MODIS Data in the Visible to Middle Infrared: First Results." *Remote Sensing of Environment* 83: 97–111.

Wagenseil, H., and C. Samimi. 2007. "Woody Vegetation Cover in Namibian Savannahs: A Modelling Approach Based on Remote Sensing." *Erdkunde* 61 (4): 325–334.

Wang, D., D. Morton, J. Masek, A. Wu, J. Nagol, X. Xiong, R. Levy, E. Vermote, and R. Wolfe. 2012. "Impact of Sensor Degradation on the MODIS NDVI Time Series." *Remote Sensing of Environment* 119: 55–61.

Wezel, A., and A. M. Lykke. 2006. "Woody Vegetation Change in Sahelian West Africa: Evidence from Local Knowledge." *Environment, Development & Sustainability* 8 (4): 553–567.

Wolfe, R. E., D. P. Roy, and E. Vermote. 1998. "MODIS Land Data Storage, Gridding, and Compositing Methodology: Level 2 Grid." *IEEE Transactions on Geoscience and Remote Sensing* 36: 1324–1338.